Chemical Science

ROYAL SOCIETY OF CHEMISTRY

EDGE ARTICLE

View Article Online
View Journal | View Issue

Cite this: *Chem. Sci.*, 2025, **16**, 20507

All publication charges for this article have been paid for by the Royal Society of Chemistry

Received 13th May 2025
Accepted 15th September 2025

DOI: 10.1039/d5sc03455h

rsc.li/chemical-science

Tracking carboplatin chemoresistance in ovarian cancer by scanning electrochemical microscopy

Roy Daou, †[a] Mengzhen Lyu,†[a] Katherine Bazin,[a] Dao Trinh,[b] Michael A. Saley,[a] Dhésmon Lima,[ac] Mark W. Nachtigal[d] and Sabine Kuss *[a]

Drug resistance in cancer presents a significant challenge in oncology, contributing to most chemotherapy failures. Early detection of drug resistance is crucial for improving treatment outcomes. Ovarian cancer is often treated with platinum-based drugs, such as carboplatin (CBDCA), but unfortunately, resistance to these compounds is common. The exact mechanisms behind platinum-based drug-resistance remain unclear. This research demonstrates the use of scanning electrochemical microscopy (SECM) to track the cellular response to chemotherpeutic exposure through the quantification of glutathione, a cellular antioxidant, as a biomarker for cellular drug resistance. In the presence of the redox mediator ferrocenemethanol, SECM successfully tracks differential cell redox behaviours in CBDCA-susceptible and CBDCA-resistant ovarian cancer cell models in response to chemotherapeutic exposure. The presented study highlights the potential of using electrochemistry to detect and quantify chemoresistance in cell samples within minutes.

Introduction

Chemoresistance is the ability of cancer cells to evade and cope with the presence of chemotherapeutics.[1] It is the leading cause of chemotherapy failures and cancer fatalities,[2] and has been reported for nearly all chemotherapeutics currently used to treat cancer. Resistance mechanisms are diverse. Efflux systems pump drug molecules out of cells before they can take action. Membrane modifications prevent molecules from diffusing into cells and intracellular mechanisms, such as enhanced metabolism or increased target expression, prevent cells from being affected by chemotherapeutic drugs. As a result, approximately 90% of cancer mortalities are directly or indirectly caused by chemoresistance.[3]

A common obstacle in epithelial ovarian cancer treatment is the development of chemoresistance to platinum-based drugs, such as carboplatin (CBDCA).[4] This platinating agent is one of the most clinically used anticancer drugs worldwide, and was introduced in chemotherapy as a strategy to decrease the toxic effects and side-effects shown by its first-generation analogous drug, cisplatin.[4] The mechanisms of action of CBDCA and cisplatin are essentially equivalent and mainly based on the formation of covalent adducts with purine DNA bases, DNA inter-strand and intra-strand crosslinks, and DNA-protein crosslink adducts[5,28] which impairs normal DNA functioning and replication, and triggers the activation of DNA-damage-mediated apoptotic pathways to suppress proliferation. In addition, it is known that the cytotoxicity of platinating agents is also promoted by an enhancement in cellular oxidative stress, which also impairs cell proliferation and triggers apoptosis.[5–7] Both CBDCA and cisplatin effectiveness at treating cancer is threatened by primary resistance mechanisms or those developed by tumour cells over time. Literature has shown that glutathione (GSH), an intracellular antioxidant, may be involved in chemoresistance mechanisms against platinum-based drugs.[8] GSH is a tripeptide composed of the amino acids cysteine, glycine, and glutamic acid which presents a crucial role at maintaining the cell's redox state by neutralizing reactive oxygen species.[8,9] Some other essential functions include the detoxification of xenobiotics and endogenous compounds, cysteine storage, and regeneration of vitamins C and E.[9] GSH can bind to platinum drugs to form stable adducts, leading to the inactivation of the drug which can no longer exert its cytotoxic effects.[10,11] Therefore, resistant cancer cells may synthesize higher GSH levels compared to non-resistant cells to cope with the presence of chemotherapeutics. In fact, several reports in the literature have shown that an enhanced GSH production can be observed in resistant cells, as reviewed by Traverso and

[a]*Laboratory for Bioanalytics and Electrochemical Sensing, Department of Chemistry, Faculty of Science, University of Manitoba, 144 Dysart Road, R3T 2N2, Winnipeg, Manitoba, Canada. E-mail: sabine.kuss@umanitoba.ca*

[b]*Laboratoire des Sciences, de l'Ingénieur pour l'Environnement (LaSIE) UMR CNRS 7356, Université de La Rochelle, Pôle Sciences et Technologie, Avenue Michel Crépeau, Cedex 1, 17042, La Rochelle, France*

[c]*Department of Chemistry and Physics, Mount Saint Vincent University, 166 Bedford Highway, B3M 2J6, Halifax, NS, Canada*

[d]*Department of Biochemistry and Medical Genetics, Rady Faculty of Health Sciences, University of Manitoba, 745 Bannatyne Avenue, R3E 0J9, Winnipeg, Manitoba, Canada*

† These authors contributed equally to the manuscript.

co-workers.[12] The association between drug resistance and increased GSH biosynthesis has also been shown to occur in ovarian cancer. For example, Godwin and colleagues demonstrated that cisplatin-resistant A2780 and A1847 ovarian cancer cell lines presented a 13- to 50-fold increase in GSH levels when compared to the original drug-susceptible cells. This study suggested that examining GSH levels is a potential indicator of clinical prognosis.[13]

Earlier chemoresistance detection improves overall treatment outcome, as alternative chemotherapeutics can be administered. However, current methods for drug resistance detection in cancer have various limitations in terms of availability, reliability, and time-efficiency.[14] For instance, to assess drug susceptibility in a sample, fresh tumour cell culture assays can take up to 7 days to give consistent results, while the 3-(4,5-dimethylthiazol-2-yl)-2,5-diphenyltetrazolium bromide (MTT) assay, a colorimetric test for assessing cell metabolic activity, requires 48–96 hours of drug exposure to cells.[15] Methods used to this end include Polymerase Chain Reaction (PCR), Western and Northern blotting, flow cytometry, and next generation sequencing.[16,17] In addition to the mentioned drawbacks, these methods do not continuously monitor cell behaviour during drug exposure. To date, no alternative methods aside from genomic and culture viability testing have been translated to clinical practice. Electrochemical methods have the potential to overcome these issues as they enable highly sensitive, rapid, and low-cost investigation and quantification of chemoresistance. SECM is a powerful electroanalytical technique that uses an ultramicroelectrode (UME) to scan a substrate while recording its electrochemical properties. The UME can move in the *X*, *Y* and *Z* direction by using a high-precision positioning system.[18] By coupling SECM with optical microscopy, electrochemical reactions taking place in close proximity to cell membranes can be monitored.[19] Due to the local detection of species, SECM is able to detect even discrete changes in the redox properties of the sample under study with high temporal resolution,[20] which makes it particularly suitable for the analysis of living biological tissue cells responding to different stimuli. SECM can effectively detect electroactive metabolites expelled by cells in real time, enabling the quantification of molecule efflux (and influx) at the single cell level.[21]

In this study, the effective application of SECM to detect CBDCA chemoresistance in living epithelial ovarian cancer cells is reported for the first time. The presented detection approach is based on the use of ferrocenemethanol ($FcCH_2OH$) as a redox mediator to assess GSH levels in drug-susceptible A2780-S and the A2780-CP platinum-resistant counterpart. To decouple the effects of cell topography and reactivity in the SECM current signal, forced convection is utilized and numerical modelling is employed.[22–24] This method enables the extraction of an apparent heterogeneous rate constant (k_0) to quantify the redox activity of the tested cell lines before and after CBDCA exposure. The results described herein demonstrate the ability of SECM to detect and quantify chemotherapeutic resistance in ovarian cancer cells for the first time. In addition, this study provides insight into the corresponding resistance mechanism.

Results and discussion

Electrochemical activity of carboplatin susceptible and resistant cell models

Previous studies suggest that epithelial ovarian cancer cells might exhibit chemoresistance towards platinum-based drugs, such as cisplatin and CBDCA, by overexpressing the enzyme γ-glutamylcysteine synthetase, which catalyses the first reaction of the biosynthetic pathway of the intracellular antioxidant GSH.[27] This leads to increased GSH production in cells presenting a resistant behaviour.[28] Due to the high chemical affinity between platinum and sulfur atoms,[29] GSH can form stable adducts with platinating agents in the intracellular environment, which detoxifies the drug.[30]

To initially examine GSH levels in living CBDCA-susceptible (A2780-S) and CBDCA-resistant (A2780-CP) cells, SECM was utilized. SECM imaging of either multiple or single-cell samples can be conducted with both 3D-imaging (Fig. 1A and B) or 2D line scans (Fig. 1C and D). To electrochemically compare A2780-S and A2780-CP cells, 3D imaging at a potential of 0.4 V (*vs.* Ag/AgCl) was carried out across cells adhered to a cell culture plate, in serum free RPMI (SF-RPMI) media containing 1 mM $FcCH_2OH$. Prior to recording line scans, an approach curve was carried out to position a 25 μm-in-diameter Pt UME near target cells. During SECM imaging across a cell, a pronounced increase in the faradaic current is recorded, which is a consequence of the continuous regeneration of the redox mediator by reduced GSH molecules exported by the cell, which is illustrated in Fig. S1. The catalytic redox loop between $FcCH_2OH$ and the reduced form of glutathione has been described in the literature.[31] At a constant potential of +0.4 V (*vs.* Ag/AgCl), the continuous oxidation of $FcCH_2OH$ to ferroceniummethanol ($[FcCH_2OH]^+$) takes place at the UME tip. GSH expelled by the cells into the extracellular medium creates a redox loop converting $[FcCH_2OH]^+$ back to its reduced form $FcCH_2OH$ (Fig. S1). The regeneration of the redox mediator generates a current increase that is observed when the UME scans over living cells. As shown in Fig. 1, no apparent difference in electrochemical current magnitude was observed qualitatively prior to the exposure to CBDCA.

To quantitatively characterize the redox activity of A2780-S and A2780-CP cells by SECM, 2D line scans were conducted in SF-RPMI media containing 1 mM $FcCH_2OH$. As it can be seen in Fig. 1C and D, the peak current in the line scans increases with the increase in the scan velocity, which is a result of a so-called "forced convection effect".[23] To compare GSH levels in CBDCA-susceptible and CBDCA-resistant cells, peak current values obtained during the line scans of both cell lines were normalized ($I_p/I_{p,i}$) and plotted against the scan velocity (Fig. 2A). This is a standard procedure to obtain a slope which accounts for cellular reactivity (the ability of cells to regenerate $FcCH_2OH$) and cellular topography.[22] Herein, I_p is defined as the peak current at each scan velocity, whereas $I_{p,i}$ is defined as the peak current at the lowest velocity (10 μm s^{-1}). The resulting slopes were taken as a measure of the cells' electrochemical response. The resulting average slopes of 0.00298 and 0.00321 for the

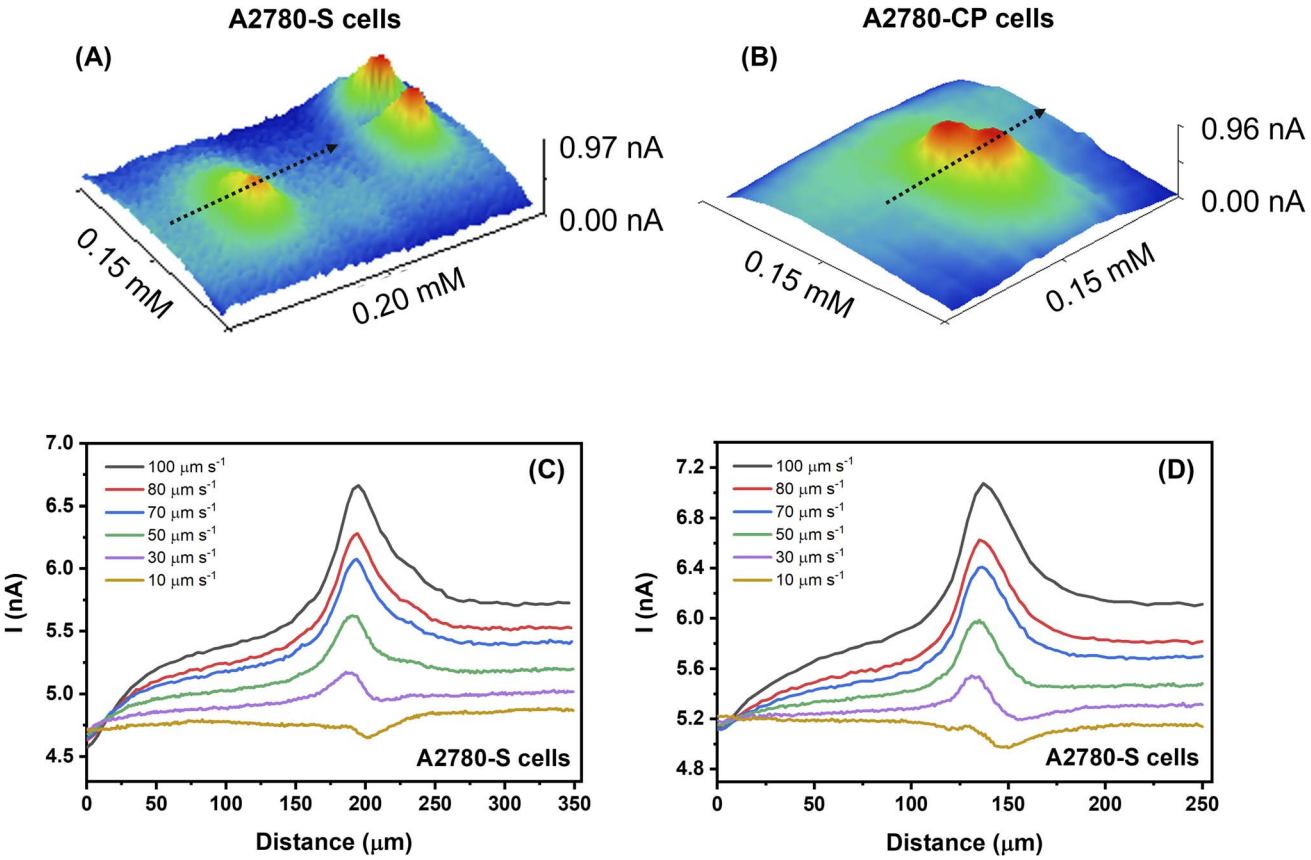

Fig. 1 SECM live cell imaging. 3D SECM imaging of living (A) susceptible A2780-S and (B) CBDCA-resistant A2780-CP ovarian cancer cells in SF-RPMI media containing 1 mM $FcCH_2OH$ at a scan velocity of 100 μm s^{-1}. SECM line scans across (C) susceptible A2780-S and (D) CBDCA-resistant A2780-CP cells in SF-RPMI media containing 1 mM $FcCH_2OH$ at scan velocities ranging from 10 μm s^{-1} to 100 μm s^{-1}.

susceptible and resistant cells lines, respectively, demonstrated no significant statistical difference when compared ($P > 0.05$). This suggests that both cell types present similar GSH levels and metabolic redox activity in the absence of CBDCA. It is important to note that while GSH is the most abundant antioxidant present in cells, minor contributions from other species cannot be ruled out.

Cell viability assay

To confirm the susceptible phenotypes and resistant phenotypes of A2780-S and A2780-CP cells towards the action of CBDCA, and to ensure that cells were viable during SECM analysis, Trypan Blue exclusion cell viability assays were performed. As expected, and shown in Fig. 2B and C, the incubation of both cell lines in RPMI media in the absence of FBS did not affect cell viability for up to 4 hours. Conducting SECM measurements in SF-RPMI is desirable due to potential electrode fouling effects caused by the presence of serum.[32] A stable viability was observed when cells were exposed to 1 mM $FcCH_2OH$, which proves that the redox mediator did not present detectable cytotoxic effects. Exposure of A2780-S cells to RPMI media containing 20 mM CBDCA and 1 mM $FcCH_2OH$ resulted in a decrease in cell viability of approximately 18% after 4 hours, whereas no significant cell death was noticed for resistant A2780-CP cells during this time. Cell viability of A2780-S cells presented a pronounced decrease after a 7 hours incubation in the presence of the drug, with a drop in cell survival of approximately 60%. At the same exposure time, A2780-CP cells only presented a 30% decrease in cell viability, which confirms a more resistant phenotype towards CBDCA compared to A2780-S. Considering that SECM measurements only take minutes to be performed, our results therefore ensure that all cells are viable during the electrochemical analysis. Importantly, the use of a high CBDCA concentration (here 20 mM) is intentional to stress cells rapidly. Given that cell viability decreases after 4 hours of incubation, it is expected that a concentration of 20 mM CBDCA affects cell metabolism and enables the detection of variations in cell redox activity using electrochemistry.

Electrochemical detection of chemoresistance in ovarian cancer cell lines A2780-S and A2780-CP based on extracellular GSH

The main chemoresistance mechanisms against platinating agents in cancer include intracellular alterations in drug metabolism, mutation of drug targets, and increased drug efflux through membrane efflux pumps.[4] In our previous study,[33] we demonstrated that the main resistance mechanism of resistant A2780-CP cells towards CBDCA is not primarily based on

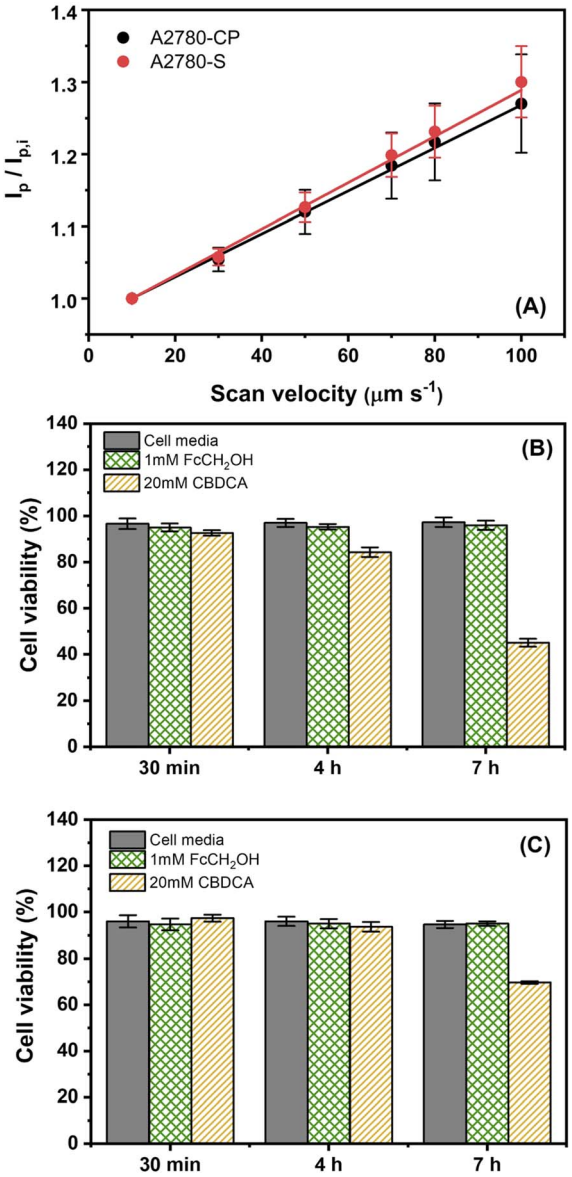

Fig. 2 (A) Dependences of normalized peak currents ($I_p/I_{p,i}$) on scan velocities ranging from 10 μm s^{-1} to 100 μm s^{-1} for susceptible and resistant model cell lines ($n = 5$ cells for each cell line). Trypan Blue cell viability assay for (B) A2780-S and (C) A2780-CP ovarian cancer model cell lines after incubation at varying time intervals in SF-RPMI media in the absence and presence of 1 mM $FcCH_2OH$ and 20 mM CBDCA ($n = 3$). Each analysis consisted of 500 cells.

increased drug efflux. Therefore, intracellular mechanisms are most likely responsible for their resistant phenotype.

Herein, the electrochemical activity of A2780-S and A2780-CP epithelial ovarian cancer cell lines exposed to 20 mM CBDCA was monitored using SECM at different scan velocities (10–100 μm s^{-1}) over a period of 60 min in SF-RPMI cell media containing 1 mM $FcCH_2OH$. After the UME had been positioned near a living cell of interest, it was horizontally scanned across the cell while recording the electrochemical current, as shown in Scheme 1. Normalized peak currents were plotted as a function of the scan velocity, and the resulting slopes were taken as a measure of cellular redox activity. A representative example of these data is depicted in Fig. 3; however, the experiment was repeated ($n = 5$) and the averages of the resultant slopes are shown in Fig. S2. Control experiments performed with susceptible A2780-S (Fig. S3A) and resistant A2780-CP cell lines (Fig. S3B) in the absence of CBDCA did not reveal significant changes in the slope of the resulting graphs (Fig. 3A and B). This indicates that $FcCH_2OH$ does not affect the metabolism of the cells, which agrees with the cell viability results previously described.

Fig. 3C and D display the normalized peak current as a function of scan velocity relationship for A2780-S and A2780-CP cell lines, immediately before (black) and after (red) exposure to 20 mM CBDCA in SF-RPMI cell media containing 1 mM $FcCH_2OH$. It is evident that, after drug exposure, the electrochemical current response of susceptible A2780-S cells dropped (Fig. 3C). In some samples, this drop remained constant over the course of the 60 min analysis time (Fig. 3C); in other samples the current continuously decreased further (Fig. S4). In contrast, resistant A2780-CP cells exhibited the opposite effect, in which both normalized peak currents, and the corresponding slopes (Fig. 3D) clearly increased after CBDCA exposure, followed by a stabilization over time. The differential current responses indicate dissimilar redox activities in A2780-S and A2780-CP cells and, therefore, different amounts of GSH that is released by each cell line upon CBDCA treatment. It is thought that after being exposed to the chemotherapeutic, A2780-S cells are unable to cope with the oxidative stress induced by CBDCA. Cell samples that demonstrated a continuous decrease in slope after CBDCA exposure detached from the cell culture plate shortly after 60 min. In contrast, A2780-CP cells are able to mitigate the cytotoxic effects induced by CBDCA. GSH presents a high binding affinity towards CBDCA to form adducts that severely attenuate the therapeutic properties of the drug. Our results are in good agreement with such observations and show that SECM can effectively detect drug resistance in epithelial ovarian cancer cell lines using GSH efflux as a chemoresistance biomarker.

The average percent variation in the normalized peak currents at 100 μm s^{-1} before and right after CBDCA exposure (0–1 min), for the A2780-S and A2780-CP cell lines (each $n = 4$), was taken as a rapid electrochemical indicator of cellular response to the drug. Such variations were compared to control experiments, in which cells were not exposed to any CBDCA. It is clear from Fig. 4A that the average normalized peak currents for the controls of both cell lines did not vary significantly during the experiment ($P > 0.05$, blue bars) when compared to the initial peak currents (grey bar). A significant decrease ($P < 0.05$) in the electrochemical signal was observed during the first minute for the susceptible A2780-S cell line after CBDCA exposure when compared to the corresponding control (red bar, A2780-S). On the other hand, resistant cells exhibited a significant increase in the current ($P < 0.05$, red bar A2780-CP) upon CBDCA exposure when compared to the control. Importantly, the average percent current variation from susceptible and resistant cells upon drug exposure also showed to be statistically different ($P < 0.01$). Based on our results, we hypothesize

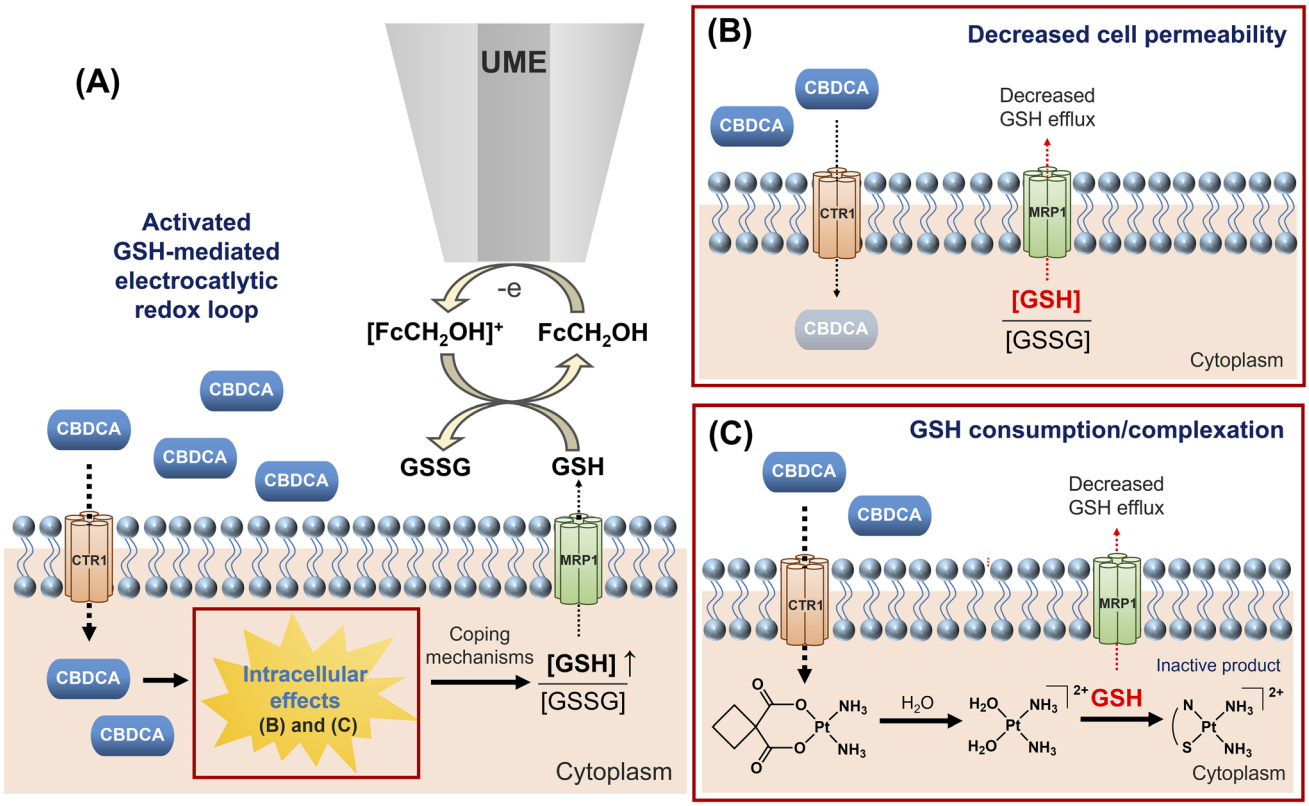

Scheme 1 Electrochemical detection of CBDCA chemoresistance in ovarian cancer cells using SECM. Resistant cells can attenuate CBDCA cytotoxic effects by (A) decreasing their membrane permeability or (B) using GSH molecules to bind to CBDCA to form inactive complexes (for clarity purposes, only part of the complex structure is represented). In both cases, a temporary decrease in GSH efflux from resistant cells is observed, which lowers cell kinetics.

that resistant A2780-CP cells have the ability to efficiently cope with CBDCA cytotoxic effects by either decreasing their membrane permeability or readily regulating GSH levels within the intracellular environment. The GSH level regulation could lead to drug detoxification by the formation of inactive adducts with CBDCA,[5] as well as to an improved cellular ability to counteract the oxidative stress generated by the drug (Scheme 1). Such changes in GSH efflux could be quickly detected using SECM. Scheme 1 presents a proposed electrocatalytic redox loop taking place at the UME tip. The differential behaviour observed when A2780-S and A2780-CP cells are compared provides evidence for the potential of SECM to rapidly distinguish between platinum-resistant and -susceptible cells.

Importantly, to understand the meaning of the observed changes in slope, different contributions to the recorded electrochemical current signal must be understood. In SECM constant-height, as employed in this study, the observed peak current is not only determined by the redox activity of the substrate, but it is also influenced by forced convection.[24,34] This is stated by the well-established mass transport equation, which governs the electrochemical current at the UME:[35]

$$J = D_j \nabla C_j - \frac{z_j F}{RT} D_j C_j \nabla \phi + C_j \boldsymbol{v}$$

As all measurements were performed at constant potential, the potential gradient term ($\nabla\phi$) is kept constant throughout the experiments. The diffusion ($D_j\nabla C_j$) and convection terms ($C_j\boldsymbol{v}$) on the other hand, are in competition with one another. At low scan rates, the former dominates, whereas at higher scan rates, the latter dominates.

The use of the slopes takes both reactivity and convective contribution of cell samples into consideration.[22,23] In short, when the UME moves past a living cell, the solution fluid is forced to flow in between the electrode tip and the cell's surface, causing the concentration of redox species in between the cell and UME to momentarily increase. As a result, the faster the UME moves, the higher is the recorded electrochemical signal. At the same time the contribution by the convection increases with increasing velocity of the UME, whereas the regeneration of the redox mediator (cell kinetics) remains constant. To better compare changes in the electrochemical current, the signal is normalized by dividing the peak currents at every scan velocity by the peak current at the slowest velocity of the UME (Fig. 3). The electrochemical current at low velocities is dominated by reactivity. Therefore, if the reactivity contribution is large (higher cell kinetics) at high velocities, the slope will appear smaller, as observed in the susceptible A2780-S cells. Oppositely, if the ability of cells to regenerate $FcCH_2OH$ through GSH efflux decreases (lower cell kinetics), the reactivity contribution

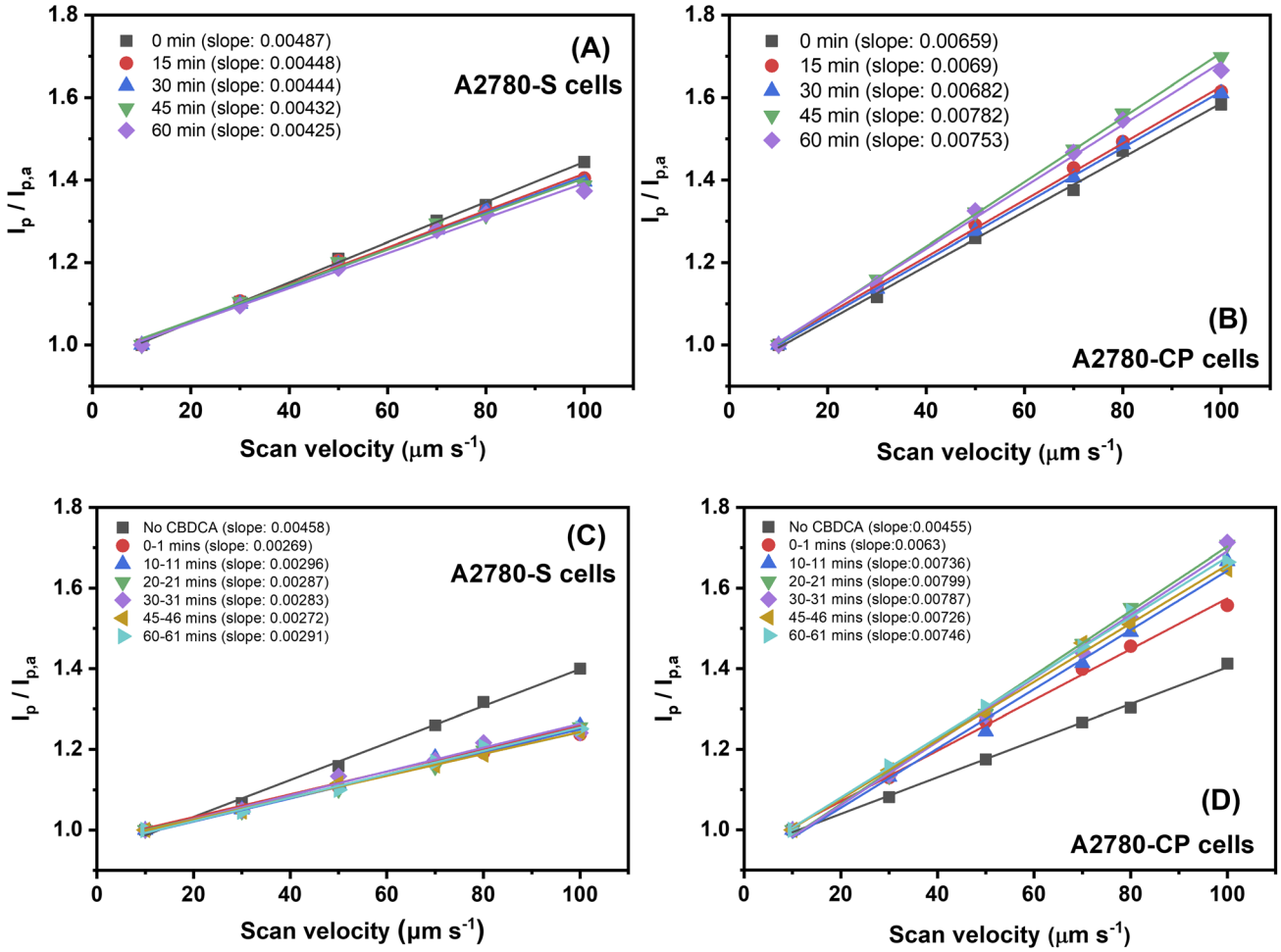

Fig. 3 Dependences of normalized peak currents ($I_p/I_{p,a}$) on scan velocities ranging from 10 μm s^{-1} to 100 μm s^{-1} for (A and C) susceptible A2780-S and (B and D) resistant A2780-CP cell lines over 60 min, in SF-RPMI media containing 1 mM $FcCH_2OH$ in the (A and B) absence and (C and D) presence of 20 mM CBDCA. These experiments were performed in quintuplicates and the corresponding slope averages can be found in the SI.

at higher velocities will be small, and the slope will appear higher, as apparent in the A2780-CP sample. As a result, the changes observed in A2780-CP mean that resistant cells efflux less GSH than their CDBCA-susceptible counterpart.

Extraction of the apparent heterogeneous rate constant (k_0) as measure for cell kinetics

Using a numerical model that simulates the impact of convection on measured current, we effectively decouple topography and reactivity contributions from the observed currents, thus allowing important information to be extracted from SECM data obtained from living cells.[23,25,26] Herein, we used a previously published numerical modelling approach[22,23] to determine the apparent heterogenous rate constant (k_0) representing the cellular kinetics of the regeneration of $FcCH_2OH$ by GSH in A2780-S and A2780-CP cells. This approach relies on the SECM constant-height imaging at low scan velocities (less than 100 μm s^{-1}) to extract a substrate's kinetic rate. The COMSOL model incorporates several experimental factors, such as microelectrode size, steady state current, scan velocity, and redox species diffusion parameters to calculate the redox environment of the cell. The normalized current experimentally determined at the UME in relation to scan velocities is fitted to theoretical results of substrate kinetic rates ranging from 10^{-8} to 10^{-1} m s^{-1}. In this approach, the kinetic rates are acquired from the normalized shear Peclet number (P_s), since the microelectrode current is influenced by the tip scan velocity, diffusion coefficient, and tip-to-sample distance.[25]

By simulating the scanning profiles for several scan speeds, an average kinetic rate, k_0, can be determined (Fig. 4B and C). Numerical simulations were conducted utilizing 5 sets of experimental data for each studied cell line. The average k_0 values determined for susceptible and resistant cells in the absence of CBDCA were $3.76 \times 10^{-6} \pm 1.97 \times 10^{-6}$ m s^{-1} and $1.52 \times 10^{-5} \pm 0.813 \times 10^{-5}$ m s^{-1}, respectively. However, after CBDCA exposure, the k_0 value for the susceptible cell line increased to $1.52 \times 10^{-5} \pm 0.711 \times 10^{-5}$ m s^{-1}, whereas the k_0 for the resistant cell line decreased to $1.09 \times 10^{-5} \pm 0.597 \times 10^{-5}$ m s^{-1}. These results mean that there is a reduction of GSH efflux from resistant A2780-CP cells, whereas GSH efflux

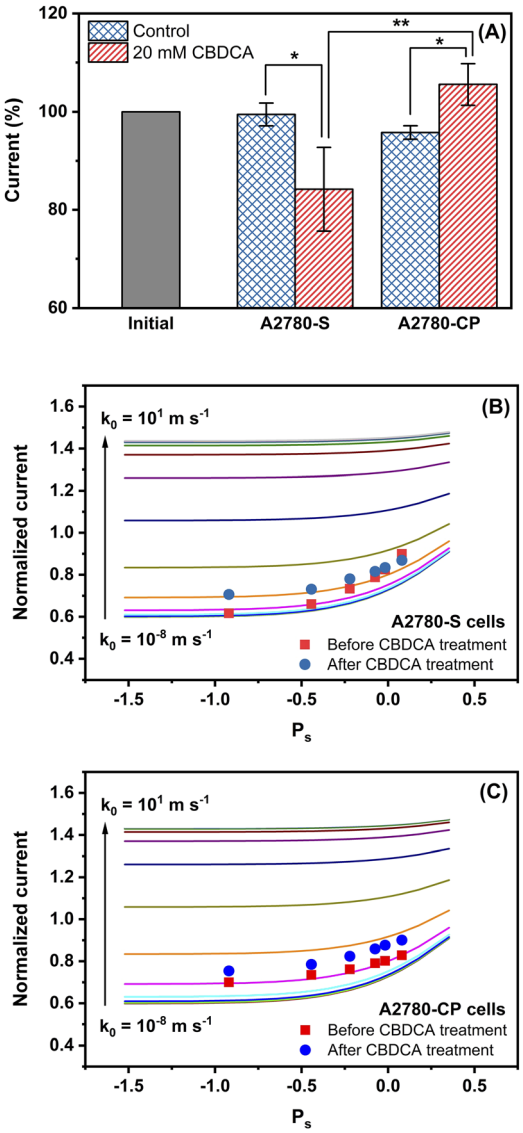

Fig. 4 (A) Average percent current variations at 100 μm s^{-1} observed for susceptible A2780-S and resistant A2780-CP cell lines during the first minute of exposure to 20 mM CBDCA (n = 4). Summary of the numerical modeling results for the analysis of (B) A2780-S and (C) A2780-CP ovarian cancer cell lines. The coloured lines depict simulated normalized peak currents for different substrate and sample kinetics ranging from 10^{-8} to 10^{1} m s^{-1}.

increases in susceptible A2780-S, which validates the conclusions presented earlier based on the slope.

Intracellular GSH detection of A2780-S and A2780-CP cell lines by flow cytometry

To propose a novel cellular mechanism of action upon CBDCA exposure, flow cytometry measurements were conducted, confirming intracellular GSH levels in A2780-S and A2780-CP cells. Herein, GSH levels were quantified by the fluorescence indicator 5-chloromethylfluorescein diacetate (CMFDA),[36] which binds to thiol groups, enabling the monitoring of intracellular GSH homeostasis. Unlike free thiol groups, metal-bound thiols do not react with CMFDA and do not contribute to fluorescence.[37,38] This difference is important as it allows the CMFDA assay to differentiate between free and metal-bound thiols, such as the GSH-Pt adducts related to CBDCA. Such differences in reactivity are often exploited in research, for example, in proteomics the CMFDA assay is applied to determine the proportion of free and metal-bound thiol-containing cysteine residues in metalloproteins.[39,40] Since GSH comprises >90% of intracellular free thiol in mammalian cells[41] the CMFDA assay applied in the current study provides accurate insight regarding differences in intracellular GSH levels when compared to eachother and when exposed to CBDCA. It should be stated that membrane permeability was not studied directly, however, the CMFDA assay provides useful data which can be used to provide insight regarding the membrane permeability.

CMFDA concentration optimization experiments were performed in the absence of CBDCA to identify its optimal concentration for flow cytometry measurements. A2780-S cells were incubated with increasing concentrations of CMFDA (0, 1.2, 1.4, 1.6, and 1.8 μM) for 15 min prior to studies. Forward scatter (FSC) and side scatter (SSC) information was visualized as dot plots (Fig. S5 A, C, E, and G) to evaluate cell morphology and population distribution. The corresponding mean fluorescence intensity was analysed and is shown as histograms (Fig. S5 B, D, F, and H) to assess CMFDA fluorescence emitted from cells. Corresponding mean fluorescence intensity in arbitrary units (a.u.) is reported as dot plots (Fig. S6) as a function of CMFDA concentrations. The results illustrated an obvious dose-dependent enhancement in fluorescence intensity with higher CMFDA concentrations. To ensure stable and reliable differentiation of intracellular GSH, while avoiding too high or low intensities that would hinder software analysis, a concentration of 1.6 μM CMFDA was chosen as optimal concentration for further measurements. In this study, 10 000 cells were analysed for each trial.

Cells without CBDCA treatment functioned as the control groups. The mean fluorescence intensity in arbitrary units (a.u.) was measured and analysed using FlowJo software. Raw intensity values of 42 242 and 36 761 were detected for A2780-S and A2780-CP untreated cells (controls), respectively. Susceptible and resistant cells resulted in values of 37 673 and 29 737 after 5 minutes incubation in 20 mM CBDCA, respectively. Both cell lines showed a decrease in fluorescence intensity compared to the controls. This experiment was carried out twice and a representative example is show in Fig. 5. Intensities from untreated cells were normalized to represent a value of 1 a.u. Accordingly, the corresponding signal intensities of treated cells were recorded as 0.892 in A2780-S cells and 0.809 in A2780-CP cells. Compared with susceptible cells, resistant cells are more sensitive to CBDCA, as evidenced by a significant drop in fluorescence intensity. These results indicate that resistant cells maintain lower intracellular GSH levels than susceptible cells after CBDCA treatment, which suggests that resistant cells consume more GSH to detoxify the cells by binding to CBDCA. This is consistent with literature regarding glutathione-S-transferase (GST) expression in the A2780-CP and A2780-S cell lines. This enzyme catalyses the conjugation of GSH-Pt

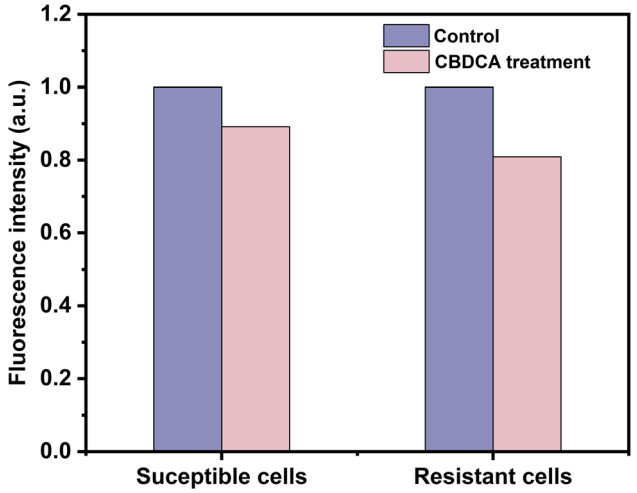

Fig. 5 Comparison of intracellular GSH levels in CBDCA-treated and untreated groups in A2780-S and A2780-CP cell lines. Signal intensity was measured by flow cytometry after 20 mM CBDCA treatment for 5 min and 1.6 μM CMFDA. Additional cytometry data is provided in Fig. S8. The number of cells studied in each experiment was 10 000.

adducts[42] and is strongly expressed in the resistant cells leading to rapid intracellular GSH consumption.[43] On the other hand, the susceptible lines poorly express GST and GSH-Pt complexation kinetics are poor,[44] resulting in higher intracellular GSH. In this study, FSC and SSC were presented as dot plots to show morphological distributions (Fig. S7 A, C, E, G) and signal intensities were analysed through histograms (Fig. S7 B, D, F, H). The repeat of this experiment under the same conditions can be seen in Fig. S8.

Conclusions

The ability of electrochemistry, and specifically SECM, to be used as a tool to detect drug resistance is herein presented at the example of epithelial ovarian cancer model cell lines. We provide evidence that SECM is a promising technique for the efficient and rapid detection of platinum-based drug resistance. SECM successfully monitored differential behaviors to drug exposure in CBDCA-susceptible and CBDCA-resistant A2780 cell lines within minutes. Based on the cellular efflux of GSH, and its direct interaction with the redox mediator $FcCH_2OH$, we observed a significant decrease in GSH efflux from resistant cells and a significant increase in GSH efflux from susceptible cells, indicating distinct variations in extracellular GSH levels. Intracellular GSH levels were measured by flow cytometry. We conclude that two possible events could be the reason for these electrochemical observations. First, upon CBDCA exposure, it is possible that resistant cells become less permeable to shield themselves from drug exposure and thereby less GSH is expelled to the cell exterior. At the same time, less permeable cells retain more intracellular GSH to enhance detoxification. Intuitively, one may surmise that intracellular GSH levels should therefore be higher in resistant cells (A2780-CP) compared to susceptible cells (A2780-S); however, the opposite is observed. This leads to the second conclusion that GSH is rapidly consumed inside resistant cells but not in susceptible cells, which is supported by the existing literature regarding glutathione-S-transferase (GST). This enzyme catalyzes the complexation of Pt-GSH adducts;[42] without GST, the reaction kinetics of this complexation are comparatively slow.[44] Research has shown that GST levels in the resistant cell line (A2780-CP) are elevated, however they are poorly expressed in susceptible cells (A2780-S).[43] It follows that the intracellular GSH consumption is significantly higher in the resistant lines, which agrees with the current study. The rapid electrochemical quantification of cellular GSH as a resistance-related biomarker, as effectively demonstrated in this study, has the potential to open the door for applications of electrochemistry, and specifically SECM, to detect drug resistance not only in epithelial ovarian cancer cells, but also in other types of cancer.

Materials and methods

Chemicals

Ferrocenemethanol ($FcCH_2OH$, $C_{11}H_{12}FeO$, >95.0%) and CDBCA ($C_6H_{12}N_2O_4Pt$, >98.0%) were acquired from TCI (USA). MicroPolish Alumina powder (1.0, 0.3, 0.05 μm) and MicroCloth Polishing pads were purchased from Buehler (USA). All media, materials and reagents for cell culture and related assays were acquired from Thermo-Fisher Scientific (USA). CMFDA was purchased from Thermo-Fisher Scientific (USA).

Cell culture

A2780-S (CDBCA-susceptible) and A2780-CP (CDBCA-resistant) cell lines were kindly provided by Dr Benjamin Tsang (University of Ottawa). Cells were cultured using RPMI-1640 medium (Gibco, Canada) supplemented with 10% (v/v) heat-inactivated fetal bovine serum (FBS), 100 units mL^{-1} penicillin and 100 μg mL^{-1} streptomycin (Gibco, Canada). Cells were cultured at 37 °C and 5% CO_2 in T-75 flasks. Prior to SECM experiments, cells were seeded into 35 mm cell culture plates and grown overnight prior to drug treatments.

Cell viability assay

To assess the viability of A2780-S and A2780-CP cells in the presence of $FcCH_2OH$ and CDBCA, Trypan Blue exclusion assays were carried out. Cells were incubated for 7 h in SF-RPMI media, SF-RPMI media containing 1 mM $FcCH_2OH$ and SF-RPMI media containing 1 mM $FcCH_2OH$ and 20 mM CP. At varying time intervals of 30 min, 1, 2, 4 and 7 h, the medium was removed, cells were washed with PBS and harvested after treatment with trypsin. Then, cells were incubated in the presence of Trypan Blue dye (1 : 1 v/v) at room temperature for 3 min.[45] Percent cells viability was determined at each time interval for each incubation condition using a Countess 2 automated cell counter (Thermo Scientific, USA).

SECM analysis

SECM measurements were performed using an EIPROScan-3 workstation and POTMASTER software (HEKA Elektronik,

GmbH, Harvard Bioscience Inc). The electrochemical setup consisted of a 25 μm-in-diameter platinum UME (RG = 2.8, HEKA Elektronik), an Ag/AgCl pseudo-reference electrode, and a 0.05 mm diameter platinum wire counter electrode integrated with a temperature controller (Warner Instruments). Prior to SECM measurements, cells were washed with PBS solution (37 °C) and incubated in serum-free RPMI-1640 cell media containing 1 mM $FcCH_2OH$ for 30 minutes at 37 °C. Target cells were identified using an inverted optical microscope located underneath the SECM stage. The approach curve was conducted above the plastic of the Petri dish but near the target cells. The UME was retracted 15 μm. Initial line scans at constant height with velocities ranging from 10 to 100 μm s^{-1} were carried out across cells. Subsequently, the electrolyte was exchanged with a fresh solution containing 20 mM CDBCA, and new line scans were performed immediately upon the exchange (0 min), and at 10, 20, 30, 45, and 60 minutes.

Numerical simulations

Mass transport and the Butler–Volmer equation were utilized to numerically simulate the electrochemical kinetics of A2780-S and A2780-CP cell lines, which was demonstrated previously.[26,34] The numerical simulation of the reported SECM experiments was carried out using a 25 μm-in-diameter Pt UME, in the presence of 1 mM $FcCH_2OH$, analysing A2780 cell lines at varying velocities from 10 to 100 μm s^{-1}.

Statistical analysis

All experiments were performed in multiples as indicated in the manuscript text. *T*-Tests were performed to evaluate statistical differences between the results obtained during SECM and cell viability assays for A2780-S and A2780-CP cell lines. Values of $P < 0.01$ and $P < 0.05$ were considered statistically significant. Due to the sample size ($n = 5$) a second non-parametric statistical analysis was carried out. Mann–Whitney *U* (two-tailed) tests were performed and found the initial population to be statistically similar to controls for both A2780-S and A2780-CP cell lines. The results also indicate that the A2780-CP and A2780-S 20 mM CBDCA treated populations were not equal to each other, nor their control experiments. Therefore, the *T*-Test and Mann–Whitney *U* test are in agreement (please find details in the SI). All statistical analyses were performed using Microsoft Excel (Microsoft Office 365).

Flow cytometry

A2780-S and A2780-CP cells were cultured at 37 °C and 5% CO_2. CMFDA was dissolved in dimethyl sulfoxide (DMSO, stock solution) and diluted in RPMI-1640 for experimental use.

CMFDA concentration optimization: A2780-S cells were washed with PBS and incubated with fresh RPMI-1640 media, or RPMI-1640 containing 1.2, 1.4, 1.6 and 1.8 μM CMFDA for 15 min. After incubation with CMFDA, cells were washed with PBS, lifted and suspended cells were centrifuged and resuspended in PBS.

To assess and compare intracellular GSH in A2780-S and A2780-CP cells with or without CBDCA treatment, both cell lines were washed with PBS and incubated with fresh RPMI-1640 media and RPMI-1640 with 20 mM CBDCA for 5 min, respectively. Cells were then washed with PBS and incubated with 1.6 μM CMFDA for another 15 min. Furthermore, cells were washed, harvested and suspended in PBS.

Flow cytometric measurements were implemented using an SH800 cell sorter from SONY Biotechnology (USA) and the recorded data was analysed with the software FlowJo, version 10.8.1.

Author contributions

RD-conducted experiments, analyzed data, wrote the manuscript. ML-conducted experiments, analyzed data, wrote the manuscript. KB- conducted experiments, analyzed data. DT-analyzed data, numerical modelling. MS-wrote the manuscript and manuscript editing DL-figure plotting, wrote the manuscript. MN-provided cell lines, scientific input and manuscript editing. SK-supervision, conceptualization of research, project administration, obtained funding, figure plotting, wrote the manuscript.

Conflicts of interest

There are no conflicts to declare.

Data availability

The data supporting this article have been included as part of the supplementary information (SI). Supplementary information is available. See DOI: **https://doi.org/10.1039/d5sc03455h**.

Acknowledgements

SK acknowledges funding by the Natural Sciences and Engineering Research Council of Canada (RGPIN-2019-05365 and RGPIN-2024-05454) for its financial support. We thank Harvard Bioscience and HEKA Electronics for continuing support. Technical contributions by Huy Tran Le Luu are also acknowledged by the authors.

Notes and references

1 G. Yeldag, A. Rice and A. Del Rio Hernandez, *Cancers*, 2018, **10**(12), 471.
2 S. T. Pan, Z. L. Li, Z. X. He, J. X. Qiu and S. F. Zhou, *Clin. Exp. Pharmacol. Physiol.*, 2016, **43**(8), 723–737.
3 A. Ramos, S. Sadeghi and H. Tabatabaeian, *Int. J. Mol. Sci.*, 2021, **22**(17), 9451.
4 G. F. Sousa, S. R. Wlodarczyk and G. Monterio, *Braz. J. Pharm. Sci.*, 2014, **50**(4), 693–701.
5 J. Zhou, Y. Kang, L. Chen, H. Wang, J. Liu, S. Zeng and L. Yu, *Front. Pharmacol*, 2020, **11**, 343.
6 F. M. Santandreu, P. Roca and J. Oliver, *Free Radicals Biol. Med.*, 2010, **49**(4), 658–666.
7 P. J. He, R. F. Ge, W. J. Mao, P. S. Chung, J. C. Ahn and H. T. Wu, *Oncol. Lett.*, 2018, **16**(6), 7131–7138.

8 H. J. Forman, H. Zhang and A. Rinna, *Mol. Aspects Med.*, 2009, **30**(1–2), 1–12.
9 V. I. Lushchak, *J. Amino Acids*, 2012, 736837.
10 J. Zhou, Y. Kang, L. Chen, H. Wang, J. Liu, S. Zeng and L. Yu, *Front. Pharmacol*, 2020, **11**, 343.
11 A. Havasi, S. S. Cainap, A. T. Havasi and C. Cainap, *Medicina*, 2023, **59**(3), 544.
12 N. Traverso, R. Ricciarelli, M. Nitti, B. Marengo, A. L. Furfaro, M. A. Pronzato, U. M. Marinari and C. Domenicotti, *Oxid. Med. Cell. Longevity*, 2013, 972913.
13 A. K. Godwin, A. Meister, P. J. O'Dwyer, C. S. Huang, T. C. Hamilton and M. E. Anderson, *Proc. Natl. Acad. Sci. U. S. A.*, 1992, **89**(7), 3070–3074.
14 T. H. Lippert, H.-J. Ruoff and M. Volm, *Int. J. Med. Sci.*, 2011, **8**(3), 245–253.
15 J. K. Wilson, J. M. Sargent, A. W. Elgie, J. G. Hill and C. G. Taylor, *Br. J. Cancer*, 1990, **62**(2), 189–194.
16 J. R. Brestoff and J. L. Frater, *J. Appl. Lab. Med.*, 2022, **7**(4), 931–944.
17 D. J. MacPhee, *J. Pharmacol. Toxicol. Methods*, 2010, **61**(2), 171–177.
18 D. Polcari, P. Dauphin-Ducharme and J. Mauzeroll, *Chem. Rev.*, 2016, **116**(22), 13234–13278.
19 I. Beaulieu, S. Kuss, J. Mauzeroll and M. Geissler, *Anal. Chem.*, 2011, **83**(5), 1485–1492.
20 A. Preet and T.-E. Lin, *Catalysts*, 2021, **11**(5), 594.
21 N. Gao, X. Wang, L. Li, X. Zhang and W. Jin, *Analyst*, 2007, **132**(11), 1139–1146.
22 S. Kuss, D. Trinh and J. Mauzeroll, *Anal. Chem.*, 2015, **87**(16), 8102–8106.
23 S. Kuss, D. Trinh, L. Danis and J. Mauzeroll, *Anal. Chem.*, 2015, **87**(16), 8096–8101.
24 S. Kuss, C. Kuss, D. Trinh, S. B. Schougaard and J. Mauzeroll, *Electrochim. Acta*, 2013, **110**, 42–48.
25 N. Thomas, D. Lima, D. Trinh and S. Kuss, *Anal. Chem.*, 2023, **95**(49), 17962–17967.
26 S. Thind, D. Lima, E. Booy, D. Trinh, S. A. McKenna and S. Kuss, *Proc. Natl. Acad. Sci. U. S. A.*, 2024, **121**(1), e2310288120.
27 T. Hibi, H. Nii, T. Nakatsu, A. Kimura, H. Kato, J. Hiratake, J. i. Oda and G. A. Petsko, *Proc. Natl. Acad. Sci. U. S. A.*, 2004, **101**(42), 15052–15057.
28 J. S. Lewis-Wambi, R. Swaby, H. Kim and V. C. Jordan, *J. Steroid Biochem. Mol. Biol.*, 2009, **114**(1), 33–39.
29 N. P. Farrell, *Chem. Soc. Rev.*, 2015, **44**(24), 8773–8785.
30 A. Potęga, *Molecules*, 2022, **27**(16), 5252.
31 S. Kuss, R. Cornut, I. Beaulieu, M. A. Mezour, B. Annabi and J. Mauzeroll, *Bioelectrochemistry*, 2011, **82**(1), 29–37.
32 A. R. Harris, P. Carter, R. Cowan and G. G. Wallace, *ChemElectroChem*, 2021, **8**(6), 1078–1090.
33 H. T. L. Luu, M. W. Nachtigal and S. Kuss, *J. Electroanal. Chem.*, 2020, **872**, 114253.
34 S. Kuss and R. G. Compton, *Electrochim. Acta*, 2017, **242**, 19–24.
35 A. J. Bard and L. R. Faulkner. in *Electrochemical methods fundamentals and applications*, Second edition, John Wiley & Sons, 2001.
36 S. Kuss, R. Cornut, I. Beaulieu, M. A. Mezour, B. Annabi and J. Mauzeroll, *Bioelectrochemistry*, 2011, **82**, 29–37.
37 M. Poot, T. J. Kavanagh, H. C. Kang, R. P. Haugland and P. S. Rabinovitch, *Cytometry*, 1991, **12**, 184–187.
38 J. Sebastia, R. Cristofol, M. Martin, E. Redriguez-Farre and C. Sanfeliu, *Cytometry, Part A*, 2002, **51A**(1), 16–25.
39 M. D. Peris-Diaz, R. Guran, O. Zitka, V. Adam and V. Krezel, *Anal. Chem.*, 2020, **92**(19), 12950–12958.
40 H. Zhong, E. Nyvltova and A. Barrientos, *Methods Mol. Biol.*, 2024, **2839**, 249–259.
41 S. K. Georgiou-Siafis and A. S. Tsiftsoglou, *Antioxidants*, 2023, **12**(11), 1953.
42 L. Sawers, M. J. Ferguson, B. R. Ihrig, H. C. Young, P. Chakravarty, C. R. Wolf and G. Smith, *Br. J. Cancer*, 2014, **111**, 1150–1158.
43 B. Gao, F. Yang, W. Chen, R. Li, X. Hu, Y. Liang and D. Li, *Oncol. Lett.*, 2019, **18**, 4262–4269.
44 D. Hagrman, J. Goodisman and A. K. Souid, *J. Pharmacol. Exp. Ther.*, 2004, **308**(2), 658.
45 W. Strober, *Curr. Protoc. Immunol.*, 2015, **111**(1), A3.B.1–A3.B.3.